CORE
Metadata, citation and similar papers at core.ac.uk
Provided by NASA Technical Reports Server

N90-28622

BEARING OPTIMIZATION FOR SSME HPOTP APPLICATION

Elizabeth S. Armstrong and Harold H. Coe
National Aeronautics and Space Administration
Lewis Research Center
Cleveland, Ohio 44135

ABSTRACT

The space shuttle main engine (SSME) high-pressure oxygen turbopumps (HPOTP) have not experienced the service life required of them. This insufficiency has been due in part to the shortened life of the bearings. To improve the life of the existing turbopump bearings, an effort is being undertaken to investigate bearing modifications that could be retrofitted into the present bearing cavity. Several bearing parameters were optimized using the computer program SHABERTH, which performs a thermomechanical simulation of a load support system. The computer analysis showed that improved bearing performance is feasible if low friction coefficients can be attained. Bearing geometries were optimized considering heat generation, equilibrium temperatures, and relative life. Two sets of curvatures were selected from the optimization: an inner-raceway curvature of 0.54, an outer-raceway curvature of 0.52, and an inner-raceway curvature of 0.55, an outer-raceway curvature of 0.53. A contact angle of 16° was also selected. Thermal gradients through the bearings were found to be lower with liquid lubrication than with solid film lubrication. As the coolant flowrate through the bearing increased, the ball temperature decreased but at a continuously decreasing rate. The optimum flowrate was approximately 4 kg/s. This paper describes the analytical modeling used to determine these feasible modifications to improve bearing performance.

INTRODUCTION

The space shuttle main engine (SSME) high-pressure oxygen turbopump (HPOTP) bearings have shown heavy wear and significant deterioration after only 10 percent of their design service time (refs. 1 and 2). Bhat and Dolan (ref. 3) attribute the shortened bearing life to the large thermally induced internal loads and the high speeds at which the bearings run. Dufrane and Kannel (ref. 2) observed heavy wear, smearing, microcracking, and pitting with operating times of less than 6000 sec. After 100- to 4000-sec total operating time, surface oxide films have been observed on the rolling element and race surfaces, indicating high surface temperatures (ref. 1). In addition, ball paths with significant wear and/or plastic deformation were present at high contact angles, indicating the presence of high axial loads (ref. 1). To improve the performance of the HPOTP bearings, Dufrane and Kannel (ref. 1) recommend modifying the bearing clearances,

the contact angle, and the outer-race clearances as well as improving cooling and lubrication.

The objective of the work described in this paper was to analyze bearing performance through computer modeling of (1) variations in raceway curvatures and contact angles, (2) variations in the lubrication method, and (3) variations in the coolant flowrate.

The computer program SHABERTH was selected to analyze the bearing design, lubrication scheme, and cooling effects in an effort to improve bearing performance. SHABERTH can simulate thermomechanical performance of a load support system for combinations of ball, cylindrical, and tapered roller bearings (ref. 4). Past studies have shown that SHABERTH can predict bearing temperatures and heat generation reasonably well (refs. 5 to 7). A model of the HPOTP bearing configuration was developed for SHABERTH. The bearing model was analyzed for both steady-state and transient conditions. All the calculations were based on the assumption that low friction coefficients could be achieved. The results from this study compare heat generation, temperature, and life data for various configurations in an effort to determine a bearing design that can withstand the harsh conditions imposed on the HPOTP bearings.

BEARING SIMULATION

The nodal system used on SHABERTH to model the 57-mm-bore ball bearing, shaft, and housing to be used in future testing is shown in figure 1. Because of symmetry, SHABERTH uses only the cross-sectional area from the shaft outward to the housing for analysis. In figure 1, nodes 1, 7, 12, and 13 are shaft nodes, nodes 2 to 5 and 8 to 11 are the bearing nodes (bearing nodes 3 and 9 are the balls, 4 and 10 are the cages, 2 and 8 are the inner races, and 5 and 11 are the outer races), nodes 6, 14, and 15 are the housing nodes, and nodes 16 to 18 are boundary nodes. These are all metal nodes. Node 19 is the air surrounding the bearing, nodes 20 to 23 are liquid oxygen (coolant) flowpaths, nodes 24 and 25 are the ambient air outside the boundaries, and node 26 is the liquid oxygen sump. Heat-transfer areas and conduction and convection paths were determined as suggested in the SHABERTH user's manual (ref. 4). Heat radiation was neglected in these calculations. Conduction paths exist between each metal node and all other metal nodes with which it has contact, between coolant nodes 20 and 22 and the bearing nodes (2 to 5 and 8 to 11), and between coolant node 21 and the shaft nodes (1, 7, 12, and 13). The path of the liquid oxygen coolant fluid flow is indicated by the dashed line in figure 1.

RESULTS AND DISCUSSION

The space shuttle main engine (SSME) high-pressure oxygen turbopump (HPOTP) bearings have shown heavy wear and significant deterioration after only 10 percent of their design service time (refs. 1 and 2). Bhat and Dolan (ref. 3) attribute the shortened bearing life to the large, thermally induced internal loads and the high speeds at which the bearings run. The computer program SHABERTH was used to calculate the performance of the HPOTP bearings. The bearing geometry and operating conditions that were varied included the raceway curvatures, the contact angle, the method of lubrication, and the coolant flowrate. The resulting rolling element fatigue life, temperature, and heat generation estimates were compared to determine performance for various operating conditions. To model the oxygen environment of the bearings, we gave all the bearing nodes initial temperatures of 90 K, the temperature of liquid oxygen at ambient pressure. Also, convective heat transfer coefficients were calculated by SHABERTH using oxygen properties (ref. 8) to determine the amount of heat transfer from the bearing nodes to the coolant nodes. It was assumed that liquid oxygen flows through the bearings for both solid and liquid lubrication cases.

Output Parameters

The primary output parameters discussed in this paper are fatigue life and temperature. SHABERTH calculates a bearing's L_{10} life, the time at which 10 percent of bearings under similar operating conditions would fail from rolling element (surface) fatigue. However, bearings seldom fail from rolling element fatigue; their failure is most often induced by improper installation, insufficient lubrication and cooling, or excessive loads. These conditions would fail a bearing before it fatigued. The life estimates in this paper are for fatigue life and, hence, are slightly optimistic. However, by comparing fatigue life estimates with various bearing parameters, trends in bearing life can be inferred. The temperature estimates from SHABERTH have compared favorably with experimental results in past work (refs. 5 and 6).

Bearing Parameters

Many bearing parameters remained fixed throughout the study. These are summarized in table I. The diameters and widths correspond with the present HPOTP bearings. The analysis assumed a shaft speed of 30 000 rpm, an axial load of 4480 N, a radial load of 6720 N per bearing, and a liquid oxygen coolant flowrate of 0.45 kg/s, except for the coolant analysis. The calculated convective heat-transfer coefficients for the coolant used liquid oxygen properties (ref. 8), table II, and those for the liquid lubricant used Freon E-1 properties (ref. 9), table III. The bearing model had 13 balls (12.7 mm in diameter) the

maximum number possible for this bearing configuration. The number of balls was maximized for the best distribution of load and for cage strength. The cage material was reinforced, glass-fiber-filled PTFE. The bearing material, for all parts except the cage, was vacuum-induction melted, vacuum-arc remelted (VIM-VAR) AISI 440C stainless steel. The material is compatible with an oxygen environment.

Geometry Optimization

The geometric parameters analyzed using SHABERTH include the raceway curvatures and the effective mounted contact angle. All geometry optimization calculations were run with liquid lubrication, Freon E-1, and liquid oxygen coolant. It was assumed that Freon E-1 was impregnated in the cage and that it lubricated the bearings. The liquid oxygen flow through the bearings was 0.45 kg/s for all geometry calculations. The raceway curvatures were varied for two effective mounted contact angles, 20° and 28°, to give an indication of trends when changing the raceway curvatures. Figure 2 shows the trends in life prediction as a function of inner-raceway curvature (f_i) for five outer-raceway curvatures (f_o). The raceway curvatures were varied from 0.52 to 0.58 in increments of 0.02. The present SSME bearing has an outer-raceway curvature of 0.53 and an inner-raceway curvature of 0.55. Figure 2(a) shows life prediction for an effective mounted contact angle of 20°, and figure 2(b) shows the life prediction for an effective mounted contact angle of 28°. Both figures demonstrate that longer life is achieved at smaller raceway curvatures.

Figure 3 shows the temperature trends as a function of inner-raceway curvature (f_i) for five outer-raceway curvatures (f_o). Figure 3(a) shows the estimated temperature of the balls for the various raceway curvatures with an effective mounted contact angle of 20°, and figure 3(b) shows the estimated ball temperature with an effective mounted contact angle of 28°. The trends on both figures indicate that a large inner-raceway curvature results in low temperatures as do the small outer-raceway curvatures. Comparing the two figures demonstrates that smaller contact angles produce lower ball temperatures than larger contact angles.

The data in figures 2 and 3 indicate that medium range inner-raceway curvatures (0.54 to 0.55) combine the benefits of low temperatures at large curvatures and long life at small curvatures. Low outer-raceway curvatures (0.52 to 0.53) were selected because they result in longer life and lower temperatures for the bearings. From these results, two sets of curvatures were selected for use when selecting the contact angle: $f_o = 0.52$, $f_i = 0.54$, and $f_o = 0.53$, $f_i = 0.55$. Another set of curvatures, $f_o = 0.54$, $f_i = 0.58$, was chosen for comparison.

Figure 4 shows the estimated fatigue life as a function of effective mounted contact angle for the three sets of curvatures. The estimated life for a particular set of curvatures increases up to a contact angle of 16° and then remains fairly constant.

The ball temperatures for various contact angles are shown in figure 5. As the contact angle increases, the ball temperature increases at an increasing rate.

From figures 4 and 5, an effective mounted contact angle between 8° and 16° would give the best bearing performance. For maximum load capacity and minimum torque, Butner (ref. 10) suggests that the contact angle be greater than 12° to 15°. Therefore, a contact angle of 16° was chosen for the preferred design.

The subsequent analyses implement the geometry configurations chosen in the geometry optimization portion of the study. Two sets of curvatures were used: $f_o = 0.52$, $f_i = 0.54$, and $f_o = 0.53$, $f_i = 0.55$. These were selected in the raceway curvature analysis. The contact angles selected were 16° and 22°. The 16° angle was selected in the contact angle analysis, and 22° is the operating contact angle of the present HPOTP bearings.

Lubrication

After determining geometry configurations for the best performance, the type of lubricant was analyzed. Most lubricants are incompatible with liquid oxygen and/or are ineffective at cryogenic temperatures (refs. 11 to 13). However, there are several possible lubricants, including liquid fluorinated polyethers (ref. 14) and certain solids (refs. 12 and 15). For the fluorinated polyethers, fluid properties (ref. 9) were written into the software so that they could be used for future work as well as in the present work. The fluorinated polyether used for this analysis was Freon E-1. Table III gives the properties for this lubricant.

Solid film lubrication coats the balls and/or raceways with a solid film that has a lower coefficient of friction than the bearing material. In SHABERTH, the solid film lubricant was modeled as dry friction with a ball-race friction coefficient reflecting the use of a coating. The friction coefficients used in this analysis were for PTFE rubbing steel. All solid film lubrication computations were calculated with liquid oxygen coolant flow.

For the transient analysis, computations were made every 0.1 sec and bearing temperatures were printed for every 1.0 sec. It was assumed that the shaft speed reaches 30 000 rpm instantaneously (within the first 0.1 sec). The analyses only include the first 30 sec of

operation because steady state was reached in all cases in that time period.

The results of the transient thermal analysis of the bearing operation for both types of lubrication is shown in figures 6 and 7. In most cases, the final, equilibrium temperature was reached in about 5 sec. The operating conditions for figures 6 and 7 are given in table I. Since the properties of the liquid lubricant, Freon E-1, were outside the range of validity of the equations in SHABERTH below 200 K, the liquid lubricated cases were run on SHABERTH with an initial temperature of 200 K. In actual testing, it would be assumed that the liquid lubricated bearings would run with dry friction from the initial temperature of 90 K, the temperature of liquid oxygen at ambient pressure, until the lubricant begins to melt. Then, the bearings would run lubricated. However, with solid film lubrication the bearings were run on SHABERTH with the coatings from the initial temperature of 90 K, which can be accurately modeled with SHABERTH.

Figures 6(a) and (b) show bearing temperatures for an f_o of 0.52, an f_i of 0.54, and an effective mounted contact angle of 16°. With liquid lubrication (fig. 6(a)), the thermal gradient between the ball and the inner race is 21 K and the thermal gradient between the ball and the outer race is 28 K. With solid film lubrication (fig. 6(b)), the thermal gradient between the ball and the inner race is 43 K and the thermal gradient between the ball and the outer race is 50 K. The thermal gradient through the bearing with liquid lubrication is 22 K less than with solid film lubrication.

Changing the effective mounted contact angle from 16° to 22° yielded a large rise in thermal gradients, as can be seen in figures 6(c) and (d). Figure 6(c) shows the thermal gradients for liquid lubrication. The difference in temperature between the ball and the inner race is 31 K and between the ball and the outer race is 40 K. In figure 6(d) temperatures for solid film lubrication are shown. The difference in temperature between the ball and the inner race is 72 K and between the ball and the outer race is 80 K. These gradients are much larger than with the smaller effective mounted contact angle of 16°.

Figures 7(a) and (b) show bearing temperatures for an f_o of 0.53, an f_i of 0.55, and an effective mounted contact angle of 16°. With liquid lubrication, thermal gradients of 20 and 27 K result between the ball and the inner race, and between the ball and the outer race, respectively (fig. 7(a)). With solid-film lubrication, thermal gradients of 39 and 45 K result between the ball and the inner race and between the ball and the outer race, respectively (fig. 7(b)).

Bearing temperatures for an f_o of 0.53, an f_i of 0.55, and an effective mounted contact angle of 22° are shown in figures 7(c)

and (d). For liquid lubrication (fig. 7(c)), the difference in temperature between the ball and the inner race is 31 K and between the ball and the outer race is 41 K. For solid film lubrication (fig. 7(d)), the difference in temperature between the ball and the inner race is 70 K and between the ball and the outer race is 78 K. These gradients are consistent with figures 7(a) and (b).

These figures, which are based on SHABERTH calculations, indicate that thermal gradients through the bearing at the ball-race contact are lower with liquid lubrication than with solid-film lubrication.

Coolant Flowrate

The flowrate was varied from 0.2 to 4.5 kg/s to determine the effect of coolant flowrate on the bearings. In figure 8, the ball temperature is shown as a function of the coolant flowrate for two geometry configurations. The flowrates are the flow through one of the bearings. As can be seen, the temperature decreases as the flowrate increases, but at a decreasing rate. From figure 8, the optimum flowrate would be approximately 4 kg/s because of diminishing returns in temperature for larger flows.

SUMMARY OF RESULTS

The bearings presently used in the high-pressure oxygen turbopump (HPOTP) of the space shuttle main engine (SSME) have a relatively short life because of the large thermally induced internal loads and the high speeds imposed upon the system. An analysis was performed to determine how these internal loads can be minimized and how the detrimental effect of the high speeds can be reduced. Several parameters can be changed in the bearing configuration for improved performance of the ball bearing. The computer program SHABERTH was selected to analyze several of these parameters: the curvature of the races, the contact angle, the coolant flowrate, and the method of lubrication. A model of the 57-mm-bore ball bearing, shaft, and housing to be used in a proposed experimental test effort was analyzed for both steady-state and transient conditions. All calculations were based on an assumption that low friction coefficients could be achieved whether solid film or liquid lubrication was used. It was assumed for all computations that liquid oxygen cooled the bearings. The results from this analysis compared temperature and fatigue life predictions for various configurations in an effort to determine a bearing design that can withstand the harsh conditions imposed on the HPOTP bearings. The following results were obtained:

1. Bearing geometries to be tested in a proposed experimental effort were optimized considering equilibrium temperatures and relative life. Outer-raceway curvatures f_o of 0.52 to 0.53 were selected

because they result in long life and low temperatures for the bearings. Inner-raceway curvatures f_i of 0.54 to 0.55 were selected because they combine the benefits of low temperatures at large inner-raceway curvatures and long life at small inner-raceway curvatures. Therefore, two sets of curvatures were selected from the optimization: $f_i = 0.54$, $f_o = 0.52$, and $f_i = 0.55$, $f_o = 0.53$. An effective mounted contact angle of 16° was selected for maximum load capacity and minimum torque. Smaller contact angles result in shorter life while larger contact angles result in higher temperatures.

2. Thermal gradients through the bearing are less with liquid lubrication than with solid film lubrication. Also, the temperature gradient through the bearing increases with increasing effective mounted contact angle.

3. As the coolant flowrate through the bearing increases, the ball temperature decreases at a decreasing rate. The optimum flowrate would be approximately 4 kg/s because of the diminishing returns in temperature for larger flows.

REFERENCES

1. Dufrane, K.F. and Kannel, J.W.: "Evaluation of SSME HPOTP Bearings from Units 2023. 2024, 6002." NASA MSFC Contract No. NAS8-36192. Task No. 121. February 27, 1987; submitted by Battelle Columbus Laboratories, Columbus, Ohio.

2. Dufrane, K.F. and Kannel, J.W.: "Evaluation of Space Shuttle Main Engine Bearings from High Pressure Oxygen Turbopump 9008," Final Report, NASA MSFC Contract NAS8-33576, Task No. 102, July 11, 1980; submitted by Battelle Columbus Laboratories, Columbus, Ohio.

3. Bhat, B.N. and Dolan, F.J.: "Past Performance Analysis of HPOTP Bearings," NASA TM 82470. March 1982.

4. Hadden, G.B. et al: Research Report - User's Manual for Computer Program AT81Y003 SHABERTH, Steady State and Transient Thermal Analysis of a Shaft Bearing System Including Ball, Cylindrical, and Tapered Roller Bearings. (SKF-AT810040, SKF Technology Services; NASA Contract NAS3-22690) NASA CR-165365, 1981.

5. Coe, H.H. and Zaretsky. E.V.: "Predicted and Experimental Performance of Jet-Lubricated 120-Millimeter-Bore Ball Bearings Operating to 2.5 Million DN," NASA TP-1196, April 1978.

6. Parker, R.J.: "Comparison of Predicted and Experimental Thermal Performance of Angular Contact Ball Bearings," NASA TP-2275, February 1984.

7. Maurer, R.E. and Pallini, R.A.: "Computer-Aided Selection of Materials for Cryogenic Turbopump Bearings," Lubrication Engineering Vol. 42, 2 pp. 78-83. February 1986.

8. Roder, H.M. and Weber, L.A.: "ASRDI Oxygen Technology Survey. Volume I: Thermophysical Properties," NASA SP-3071, 1972.

9. FREON E Series Fluorocarbons. Dupont Technologies Bulletin EL-8B, 1967.

10. Butner, M.F. and Keller, R.B.: "Liquid Rocket Engine Turbopump Bearings." NASA SP-8048, March 1971.

11. Scibbe, H.W.: "Bearings and Seals for Cryogenic Fluids", SAE paper #680550, November 13, 1967.

12. Scibbe, H.W., Brewe, D.E., and Coe, H.H.: "Lubrication and Wear of Ball Bearings in Cryogenic Hydrogen." NASA TM X-52476, September 1968.

13. Dietrich, M.W., Townsend, D.P., and Zaretsky, E.V.: "Rolling-Element Lubrication with Fluorinated Polyether at Cryogenic Temperatures (160 to 410 °R)," NASA TN D-5566. November 1969.

14. Dietrich, M.W. and Zaretsky, E.V.: "Effect of Viscosity on Rolling Element Fatigue Life at Cryogenic Temperatures with Fluorinated Ether Lubricants," NASA TN D-7953, April 1975.

15. Brewe, D.E., Scibbe, H.W., and Anderson, W.J.; "Film-Transfer Studies of Seven Ball-Bearing Retainer Materials in 60 °R (33 °K) Hydrogen Gas at 0.8 Million DN Value," NASA TN D-3730, November 1966.

FIGURE CAPTIONS

Figure 1. - Nodal system and coolant flow path used to model the 57-mm-bore bearing, shaft, and housing.

(a) Effective mounted contact angle, 20°.

(b) Effective mounted contact angle, 28°.

Figure 2. - Bearing fatigue life as a function of raceway curvature. Shaft speed, 30 000 rpm; thrust load, 4450 N; radial load, 6720 N per bearing; lubricant, Freon E-1; coolant flowrate, 0.45 kg/s.

(a) Effective mounted contact angle, 20°.

(b) Effective mounted contact angle, 28°.

Figure 3. - Ball temperature as a function of raceway curvature. Shaft speed, 30 000 rpm; thrust load, 4450 N; radial load, 6720 N per bearing; lubricant, Freon E-1; coolant flowrate, 0.45 kg/s.

(a) Effective mounted contact angle, 20°.

(b) Effective mounted contact angle, 28°.

Figure 4. - Bearing fatigue life as a function of effective mounted contact angle. Shaft speed 30 000 rpm; thrust load, 4450 N; radial load, 6720 N per bearing; lubricant, Freon E-1; coolant flowrate, 0.45 kg/s.

Figure 5. - Ball temperature as a function of effective mounted contact angle. Shaft speed, 30 000 rpm; thrust load, 4450 N; radial load, 6720 N per bearing; lubricant, Freon E-1; coolant flowrate, 0.45 kg/s.

Figure 6. - Bearing temperature as a function of time for an outer-raceway curvature of 0.52 and an inner-raceway curvature of 0.54. Shaft speed, 30 000 rpm; thrust load, 4450 N; radial load, 6720 N per bearing; coolant flowrate, 0.45 kg/s.

(a) Liquid lubrication, Freon E-1; contact angle, 16°.

(b) Solid lubrication, PTFE; contact angle, 16°.

(c) Liquid lubrication, Freon E-1; contact angle, 22°.

(d) Solid lubrication, PTFE. Contact angle = 22°.

Figure 7. - Bearing temperature as a function of time for an outer-raceway curvature of 0.53 and an inner-raceway curvature of 0.55. Shaft speed, 30 000 rpm; thrust load, 4450 N; radial load, 6720 N per bearing; coolant flowrate, 0.45 kg/s.

(a) Liquid lubrication, Freon E-1; contact angle, 16°.

(b) Solid lubrication, PTFE; contact angle, 16°.

(c) Liquid lubrication, Freon E-1.

(d) Solid lubrication, PTFE.

Figure 8. - Ball temperature as a function of coolant flowrate. Shaft speed, 30 000 rpm; thrust load, 4450 N; radial load, 6720 N per bearing; lubricant, PTFE.

TABLE I. - FIXED BEARING PARAMETERS[a]

Bore diameter, d_b, mm	57
Pitch diameter, d_e, mm	80.5
Cage-land diameter, d_{cl}, mm	86.9
Outside outer-race diameter, d_a, mm	103
Cage width, mm	18.7
Bearing width, mm	19.5
Shaft speed, rpm	30 000
Axial load, N	4480
Radial load, N	6720
Coolant flowrate[b], kg/s	0.45

[a]See figure 1.
[b]Not applicable to coolant flowrate analysis.

TABLE II. - OXYGEN PROPERTIES AT ATMOSPHERIC PRESSURE[a]

	Temperature, K	
	90	200
Density, kg/m^3	1140.9	1.955
Conductivity, w/m °C	0.1516	0.01824
Specific heat, kJ/kg °C	1.717	0.9131
Dynamic viscosity, m^2/s	1.196×10^{-3}	1.48×10^{-5}
Kinematic viscosity, kg/m-s	0.171×10^{-6}	7.59×10^{-6}

[a]Reference 20.

TABLE III. - FLUORINATED POLYETHER E-1 PROPERTIES AT ATMOSPHERIC PRESSURE[a]

	Temperature, K	
	200	298
Density, kg/m^3	1820	1540
Conductivity, w/m °C	0.0839	0.0649
Specific heat, kJ/kg °C	(b)	1.034
Dynamic viscosity, kg/m-s	4.0×10^{-3}	0.5×10^{-3}
Kinematic viscosity, m^2/s	2.2×10^{-6}	0.3×10^{-6}

[a]Reference 20.
[b]Not available in reference 20.

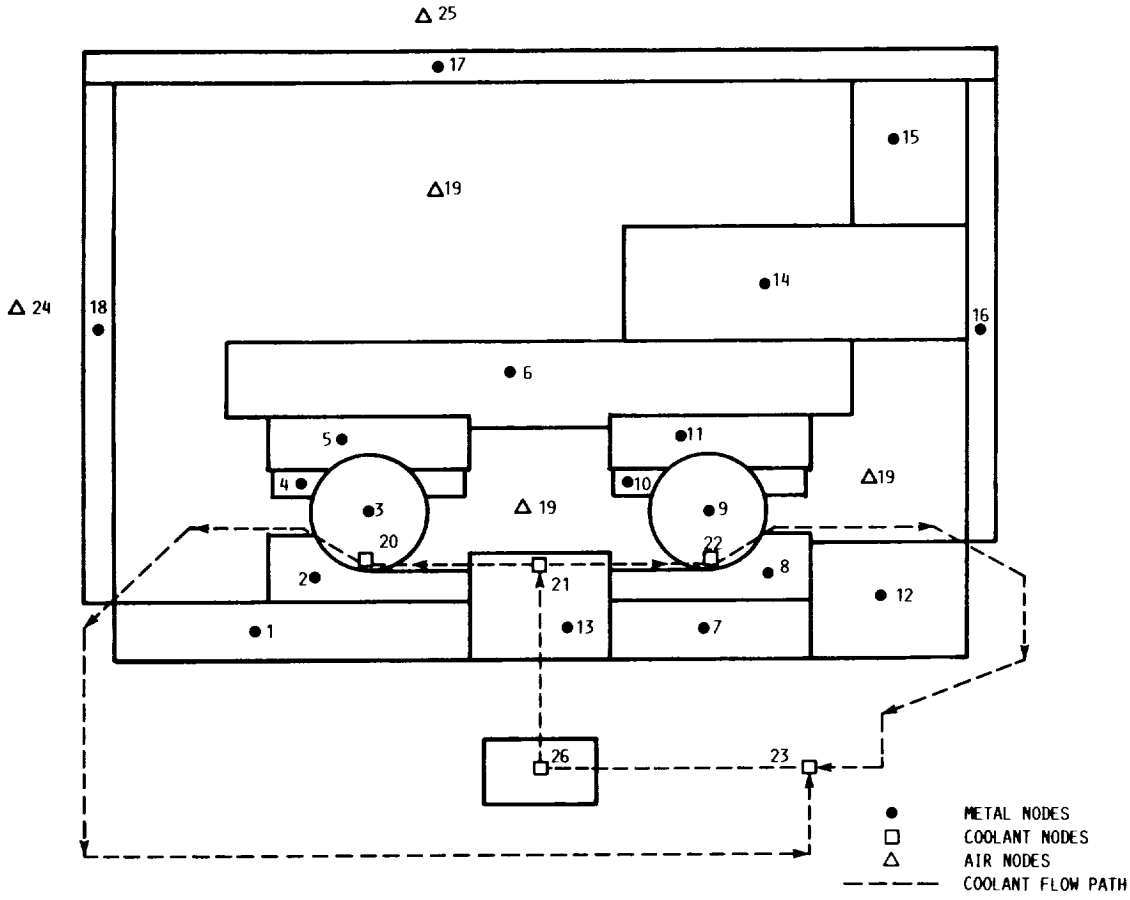

FIGURE 1. - NODAL SYSTEM AND COOLANT FLOW PATH USED TO MODEL THE 57-MM-BORE BEARING, SHAFT, AND HOUSING.

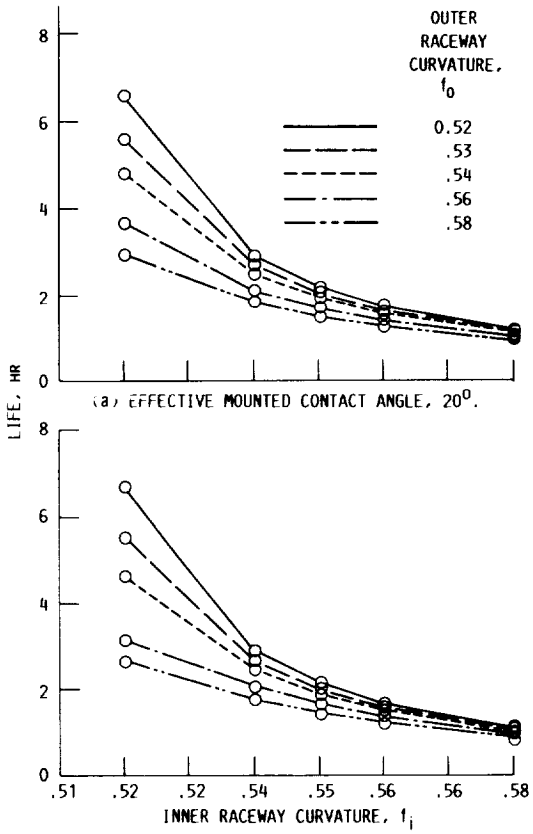

(a) EFFECTIVE MOUNTED CONTACT ANGLE, 20^o.

(b) EFFECTIVE MOUNTED CONTACT ANGLE, 28^o.

FIGURE 2. - BEARING FATIGUE LIFE AS A FUNCTION OF RACEWAY CURVATURE. SHAFT SPEED, 30 000 RPM; THRUST LOAD, 4450 N; RADIAL LOAD, 6720 N PER BEARING; LUBRICANT, FREON E-1; COOLANT FLOWRATE, 0.45 KG/S.

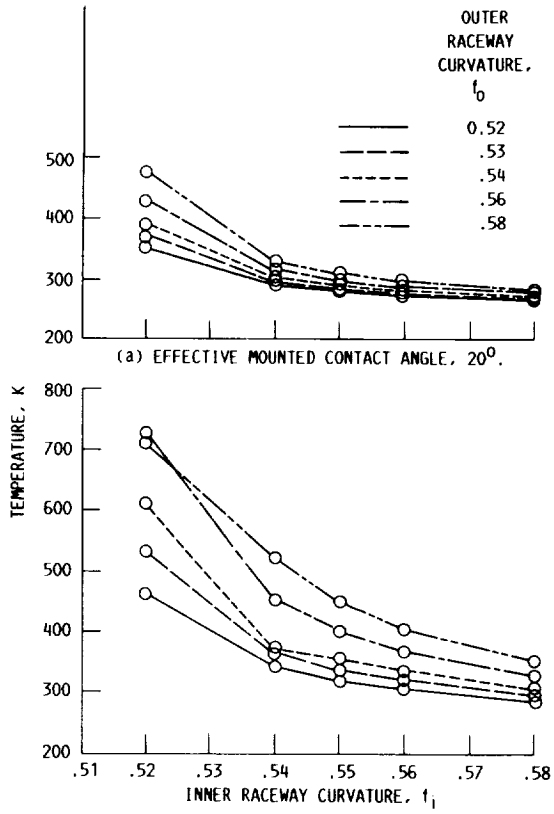

(a) EFFECTIVE MOUNTED CONTACT ANGLE, 20^o.

(b) EFFECTIVE MOUNTED CONTACT ANGLE, 28^o.

FIGURE 3. - BALL TEMPERATURE AS A FUNCTION OF RACEWAY CURVATURE. SHAFT SPEED, 30 000 RPM; THRUST LOAD, 4450 N; RADIAL LOAD, 6720 N PER BEARING; LUBRICANT, FREON E-1; COOLANT FLOWRATE, 0.45 KG/S.

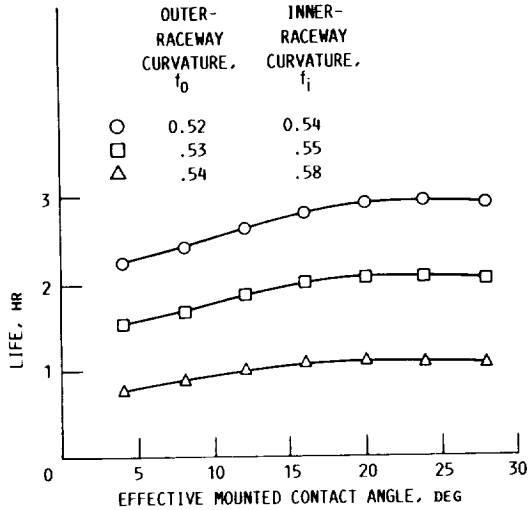

FIGURE 4. - BEARING FATIGUE LIFE AS A FUNCTION OF EFFECTIVE MOUNTED CONTACT ANGLE. SHAFT SPEED, 30 000 RPM; THRUST LOAD, 4450 N; RADIAL LOAD, 6720 N PER BEARING; LUBRICANT, FREON E-1; COOLANT FLOWRATE, 0.45 KG/S.

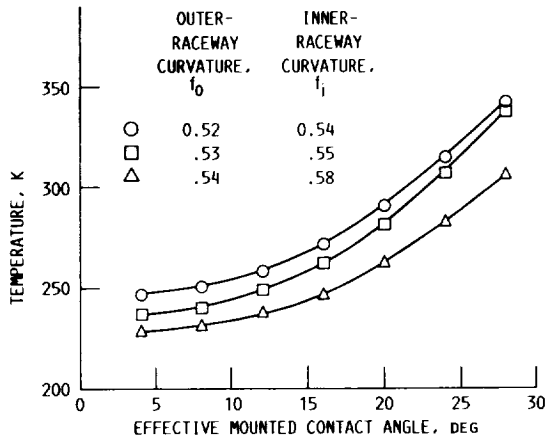

FIGURE 5. - BALL TEMPERATURE AS A FUNCTION OF EFFECTIVE MOUNTED CONTACT ANGLE. SHAFT SPEED, 30 000 RPM; THRUST LOAD, 4450 N; RADIAL LOAD, 6720 N PER BEARING; LUBRICANT, FREON E-1; COOLANT FLOWRATE, 0.45 KG/S.

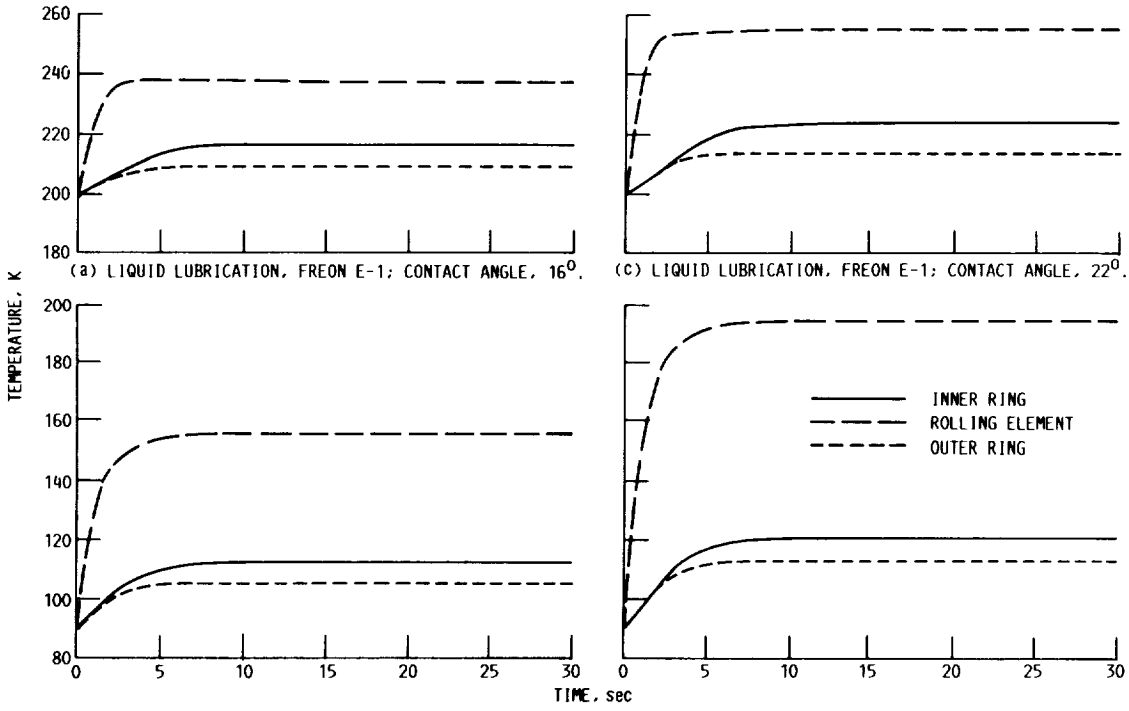

FIGURE 6. - BEARING TEMPERATURE AS A FUNCTION OF TIME FOR AN OUTER-RACEWAY CURVATURE OF 0.52 AND AN INNER-RACEWAY CURVATURE OF 0.54. SHAFT SPEED, 30 000 RPM; THRUST LOAD, 4450 N; RADIAL LOAD, 6720 N PER BEARING; COOLANT FLOWRATE, 0.45 KG/S.

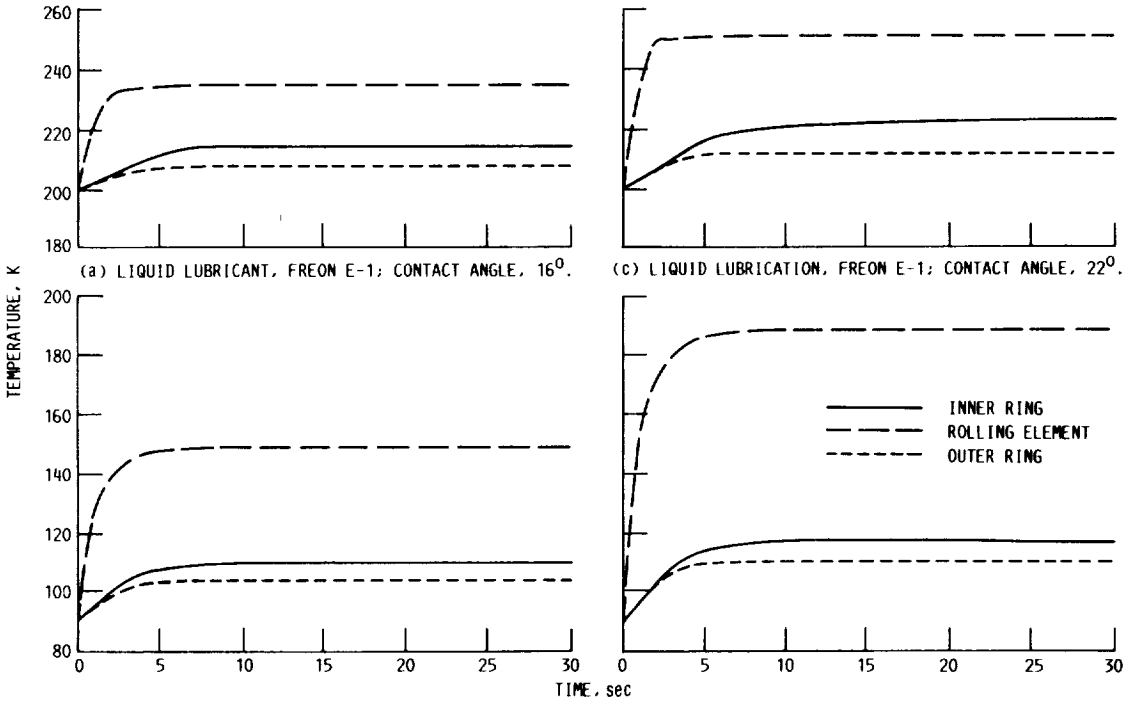

FIGURE 7. - BEARING TEMPERATURE AS A FUNCTION OF TIME FOR AN OUTER-RACEWAY CURVATURE OF 0.53 AND AN INNER-RACEWAY CURVATURE OF 0.55. SHAFT SPEED, 30 000 RPM; THRUST LOAD, 4450 N; RADIAL LOAD, 6720 N PER BEARING; COOLANT FLOWRATE, 0.45 KG/S.

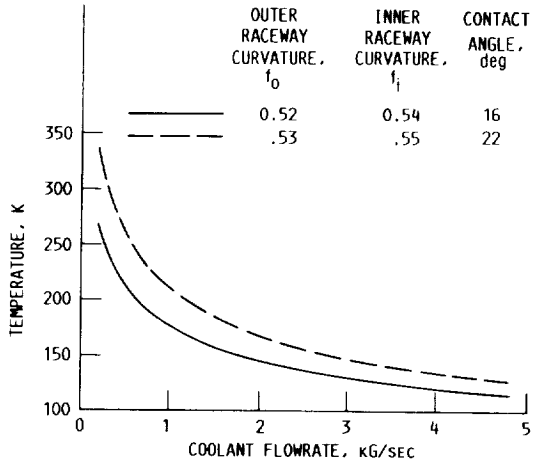

FIGURE 8. - BALL TEMPERATURE AS A FUNCTION OF COOLANT FLOWRATE. SHAFT SPEED, 30 000 RPM; THRUST LOAD, 4450 N; RADIAL LOAD, 6720 N PER BEARING; LUBRICANT PTFE.